Geomechanics and Engineering, *Vol. 34, No. 5 (2023) 561-575*
https://doi.org/10.12989/gae.2023.34.5.561

A hybrid approach to predict the bearing capacity of a square footing on a sand layer overlying clay

Erdal Uncuoğlu[a], Levent Latifoğlu[b] and Zulkuf Kaya*

Department of Civil Engineering, Erciyes University,
Koşk District, Ahmet El Biruni Stress, 38030, Melikgazi, Kayseri, Turkey

(*Received February 6, 2023, Revised August 2, 2023, Accepted August 5, 2023*)

Abstract. This study investigates to provide a fast solution to the problem of bearing capacity in layered soils with easily obtainable parameters that does not require the use of any charts or calculations of different parameters. Therefore, a hybrid approach including both the finite element (FE) method and machine learning technique have been applied. Firstly, a FE model has been generated which is validated by the results of in-situ loading tests. Then, a total of 192 three-dimensional FE analyses have been performed. A data set has been created utilizing the soil properties, footing sizes, layered conditions used in the FE analyses and the ultimate bearing capacity values obtained from the FE analyses to be used in multigene genetic programming (MGGP). Problem has been modeled with five input and one output parameter to propose a bearing capacity formula. Ultimate bearing capacity values estimated from the proposed formula using data set consisting of 20 data independent of total data set used in MGGP modelling have been compared to the bearing capacities calculated with semi-empirical methods. It was observed that the MGGP method yielded successful results for the problem considered. The proposed formula provides reasonable predictions and efficient enough to be used in practice.

Keywords: finite element method; layered soils; loading test; multigene genetic programming; ultimate bearing capacity

1. Introduction

The formation of the failure mechanism and consequently the ultimate bearing capacity of shallow foundations resting on a sand layer overlying clay are significantly affected by the relative strengths (c_u and ϕ') of the sand and clay layers, the thickness of the upper sand layer (H) and surcharge pressure (q_0). The conventional bearing capacity theories can successfully estimate the ultimate bearing capacity in the homogeneous soil conditions while they cannot be applied such types of problems where soil properties vary with depth. An exact analytical bearing capacity model with a comprehensive understanding of the footing-soil interaction is still not available due to the complexity of the problem. Geotechnical engineers mainly estimate the ultimate bearing capacity of the foundations on a sand layer overlying clay using either the semi-empirical bearing capacity models based on limit equilibrium method or numerical analysis methods. The majority of the more recently studies on the bearing capacity of the shallow foundations have focused on the predicting the bearing capacity in layered soils (Uncuoğlu 2015, Mosallanezhad and Moayedi 2017, Tang *et al.* 2017, Eshkavari 2018, Eshkavari *et al.* 2019, Zheng *et al.* 2019, Zheng *et al.* 2019, Askari *et al.* 2021, Pham and Ohtsuka 2021). In these studies, analytical approaches based on limit equilibrium method, different numerical solutions (e.g. finite element method, finite element limit analysis, rigid-plastic finite element method etc.), statistical analysis methods and artificial intelligence techniques have been used. It is aimed to overcome the shortcomings existing in the semi-empirical conventional bearing capacity models by improving the simplified failure mechanisms, modifying the model and eliminating the uncertainties.

In practice, the ultimate bearing capacity of a rigid footing on a sand layer overlying clay is estimated using the Projection Area Method (PAM) (Terzaghi and Peck 1948), Punching Shear Method (PSM) (Meyerhof 1974, Hanna and Meyerhof 1980) and Okamura *et al.* (1998) model (OM). The solution is obtained based on the assumed simplified failure mechanism and the equilibrium of forces. The failure mechanisms assumed in these methods have been defined based on the results obtained from *1g* and *ng* laboratory model tests. It is generally assumed that an imaginary rigid sand block between the footing base and the interface of the sand and clay is pushed into the clay together with the footing, a punching shear failure in upper sand layer and a general shear failure in the lower clay layer. The vertical stress on the base of the sand block is assumed as equal to the bearing capacity of a rigid footing with rough base on the lower clay subjected to a surcharge pressure. The ultimate bearing capacity is calculated using the equilibrium of the forces acting on the sand block.

These methods can produce different bearing capacity

*Corresponding author, Associate Professor
E-mail: zkaya@erciyes.edu.tr
[a]Associate Professor
E-mail: erdalu@erciyes.edu.tr
[b]Assistant Professor
E-mail: latifoglu@erciyes.edu.tr

ISSN: 2005-307X (Print), 2092-6219 (Online)

values from each other due to the assumptions made in the methods, the contribution of the shearing resistance along the side surface of the sand block and the uncertainties arising from the experimental coefficients used. In the PAM, it is assumed that the load spreading angle, α, is constant independent of the relative strength of the two soil layers and geometrical conditions (*H/B*). Moreover, there is doubt on the failure mechanism since the contribution of the sand layer to the bearing capacity is not taken into account. Meyerhof (1974), Hanna and Meyerhof (1980) and Hanna (1981) proposed the PSM in which the value of α is equal to 0. The shearing resistance along the vertical side surface of the block is taken into account using the punching shear coefficient, K_s. The K_s coefficient is defined from the charts as a function of the strength ratio of the sand and clay layers and the internal friction angle of the sand. But, there is an obligation to make the interpolation or extrapolation for values out of the values defined in the design charts. In addition, the use of K_s coefficient which is valid only for a limited range of material properties causes uncertainties on the estimated bearing capacity values. Okamura *et al.* (1998) developed a model considering that the load spreading angle α changes with both the strength of the lower clay layer and the thickness of the upper sand layer. However, the shearing resistance along the side surfaces of the sand block was also taken into account using the passive earth pressure coefficient, K_p. Okamura *et al.* (1998) stated that the proposed bearing capacity model is applicable for certain value ranges of the normalized bearing capacity of the lower clay layer, λ_c and surcharge pressure, λ_p ($\lambda_c \leq 26$ and $\lambda_p \leq 4.8$). The mentioned analytical bearing capacity methods based on limit equilibrium approach have been developed interpreting the results of laboratory model tests where the material properties were in limited range. It is generally accepted that these methods can be applied for the problems having different geometries and soil properties out of the experimentally tested ranges. But there are doubts about the failure mechanisms how valid for these cases. Predictions of the bearing capacity by such semi-empirical analytical models should be considered as the first estimate of the failure load. In these methods the deformation behavior of the system and the developing of the deformations are not taken into account. Therefore, it is needed to know at which displacement value the estimated bearing capacity obtained. On the other hand, the characteristics of load-settlement curves depend on the failure mode cannot be evaluated considering the progressive failure process. It cannot be known how the relative strength of the two layers and geometrical conditions of the problem change the failure mechanism.

There is still no a bearing capacity model considering the behavior of layered soils for the cases that can be encountered in practice having material properties in a wide range and different problem geometries with a well-understood footing-soil interaction.

In the analyses carried out by Finite Element Method (FEM), the problem geometry is evaluated as a whole. The failure condition is reached by the resulting deformation behavior depending on the various factors such as the thickness of the sand layer, relative density of the sand, the undrained shear strength of the clay, groundwater level, loading conditions, material models, mesh size etc. However, the different deformation characteristics of the two layer and the undrained shear strength of the lower clay will affect the value of mobilized internal friction angle ($\phi_{mobilized}$) in the upper sand layer and therefore the bearing capacity of the layered soil. Hence, there is no a certain failure mechanism. In FEM analyses, if the failure condition is not reached under the applied load, the ultimate bearing capacity is defined using the load corresponding a displacement criterion.

Artificial Intelligence (AI) techniques are efficient and powerful tools to process of datasets including large amounts of data and to find complex and highly non-linear relationships among different parameters. Machine Learning (ML) is a branch of the AI able to learn through data analysis, sample perceptions and allows machines to develop human-like intelligence without need for special programming. In recent years, ML techniques are so popular in solving geotechnical engineering problems such as soil classification (Bhattacharya and Solomatine 2006, Kovacevic *et al.* 2010, Bonini *et al.* 2017, Carvalho and Riberio 2019), soil profiling (Arel 2012), soil liquefaction (Juang and Chen 1999, Hanna *et al.* 2007, Goh and Goh 2007, Livingston *et al.* 2008, Kohestani *et al.* 2015), slope stability (Ferentinou and Sakellariou 2007, Bui *et al.* 2019, Maxwell *et al.* 2020), foundation settlement (Samui 2008, Nejad *et al.* 2009, Nejad and Jaksa 2017, Vu Luat *et al.* 2020, Sasmal and Behera 2021), bearing capacity (Laman and Uncuoğlu 2009, Gomes *et al.* 2021, Uncuoğlu *et al.* 2022), the coefficient of lateral earth pressure at rest (Uncuoğlu *et al.* 2008, Uncuoğlu *et al.* 2021). The studies mentioned above achieved reasonable results for the proposed problems.

In geotechnical engineering problems, it is very important to make realistic predictions of the behavior of a prototype. But it is so difficult and expensive to obtain data from the loading tests performed in-situ conditions in prototype scale. On the other hand, laboratory model studies have a number of disadvantages due to the loading and drainage conditions, initial stress state, sampling and errors meeting during the experiments.

In the present study, an equation has been developed to predict the ultimate bearing capacity of a square footing on a sand layer overlying clay. In the proposed bearing capacity equation, the footing-soil interaction, load-settlement relationship, the entire of the soil profile are considered and it does not require the use of any charts or graphic. The steps followed are summarized in the below.

- The full-scale loading tests conducted by Briaud and Gibbens (1997) on square footings resting on sand soil have been modelled and analyzed using the FEM. With this way, a calibrated and validated finite element model has been created to be used in the generation of the data set.
- A data set has been created using the results obtained from a total of 192 three-dimensional finite element analyses performed for different footing sizes, different sand densities, different undrained shear strengths and different *H/B* ratios. It can be said that the value ranges

used belonging to the parameters in the data set represent the many situations that can be encountered in practice.

- The created data set has been modelled by Multi-Gene Genetic Programming (MGGP) method which is a ML technique to develop a bearing capacity equation that predicts the ultimate bearing capacity of a square footing on a sand layer overlying clay.
- The reliability of the proposed equation was tried by a data set consisting of 20 data independent of the total data set used in MGGP modelling. The estimated ultimate bearing capacity values by proposed bearing capacity equation using the data in the validation data set were compared to the bearing capacity values calculated using the semi-empirical equations proposed by Meyerhof (1974), Hanna and Meyerhof (1980) and Okamura *et al.* (1998).

The methodology used in the study and proposed bearing capacity equation represent the innovative aspect of the study. The proposed equation provides reasonable predictions and efficient enough to be used in practice.

2. Finite element modelling

In this study, numerical analyses have been carried out with commercial Finite Element (FE) code Plaxis 3D. The analyses have been performed in two stages named as validation analyses and layered soil analyses. In the validation analyses, the full-scale loading tests conducted by Briaud and Gibbens (1997) have been modelled to obtain a model that produces reliable results for the layered soil analyses. The layered soil analyses have been carried out to investigate the effects of various parameters on the bearing capacity of square footings on a sand layer overlying clay. A data set including results obtained from layered soil analyses has been created to be used in ML modelling.

Briaud and Gibbens (1997) conducted loading tests on square spread footings ranging in size from 1.0 m to 3.0 m to investigate the effects of footing size on bearing capacity and settlement behavior. The embedment depth of footings was 0.76 m. The load value causing 150 mm of settlement was accepted as the failure load. The test site soil profile consists of silty sand layer to a depth of 11.0 m followed by a stiff clay layer which extends until a depth of at least 33.0 m. The groundwater level was a depth of 4.9 m from the ground surface. Sandy soil has been evaluated as lightly overconsolidated due to the dessication of the fines and removal of about 1.0 m of overburden at the location of test site.

Accuracy of the finite element model to be used in the layered soil analyses was demonstrated minimizing the difference between the load-settlement curves obtained from analyses with experimental ones. Boundaries and depth of the model geometry, mesh density, type of loading and generation of initial stress state to be used in FE analyses were taken into consideration during the validation process. The properties of the sand soil (BG-Sand) used in validation analyses were obtained from the site characterization and laboratory tests provided in Briaud and Gibbens (1997). Thereafter, this sand also used in the layered soil analyses to model the relatively loose sand condition while the relatively dense sand condition was simulated using the properties of Seyhan River Sand (LY-Sand) obtained from the study done by Laman and Yildiz (2007). It was assumed that both sand and clay layer are normally consolidated in the analyses performed in layered conditions.

Table 1 HS model parameters for BG-Sand soil used in validation analyses

Parameter	Value
Unit weight, γ_n (kN/m³)	15.65
Friction angle, ϕ (°)	36.40
Cohesion, c (kN/m²)	0.30
Dilatancy angle, ψ (°)	4.00
Secant stiffness, $E_{50}^{ref.}$ (kN/m²)	14600
Unloading/reloading stiffness, $E_{ur}^{ref.}$ (kN/m²)	43800
Oedometer stiffness, $E_{oed.}^{ref.}$ (kN/m²)	14600
Unloading/reloading poission ratio, ν_{ur}	0.20
Reference stress for stiffness, $p^{ref.}$ (kN/m²)	100
Power, m	0.50
Failure ratio, R_f	0.90
The coeficient of lateral earth pressure at rest, K_0^{nc}	0.407
Preoverburden pressure, POP (kN/m²)	362.50
Over Consolidation Ratio, OCR	1

The deformation characteristics of soils are functions of effective stress state, relative density, strain level and stress-strain history. Mechanical properties of sand soils involving stress-strain-dilatancy behaviour are affected significantly by the variation of confining pressure. The real soil behaviour is non-linear. In other words, the soil stiffness is not constant and changes depending on the stress level within the soil mass. In the Hardening Soil (HS) model, the soil behaviour can be modelled much more accurately using three different soil stiffness moduli. HS model also takes into account the stress dependency state of soil stiffness moduli and dilatancy behaviour of sand soil. The yield surface can expand due to plastic strains. In advanced soil models such as HS model, loading history could be taken into account by using overconsolidation ratio (OCR) or pre-overburden pressure (POP). The HS model uses non-associated flow rule together with a plastic potential function that takes into account the difference between the internal friction angle and the dilation angle (Lo Presti *et al.* 1995, Maeda and Miura 1999, Plaxis 3D 2012, Tjie-Liong 2014). The nonlinear behavior of sand soil was modelled using the HS model due to the reasons mentioned above. The HS model parameters used in the finite element analyses are shown in Tables 1 and 2.

The drained condition was assumed for the sands. Reference confining pressure is used as equal to $p_{ref.}$=100 kN/m². The actual stiffness depends on minor principal stress σ'_3. The stiffness modules used in HS model are stress-dependent and the magnitude of stress dependence is taken into account using the m exponent value. The $E_{50}^{ref.}$, $E_{ur}^{ref.}$ and $E_{oed}^{ref.}$ are the stiffness parameters corresponding to reference pressure. The $E_{50ref.}$ is used to model the plastic deformations occurred during the primary deviatoric

Table 2 HS model parameters for sand soils used in layered soil analyses

Parameter	BG-Sand	LY-Sand
Unit weight, γ_n (kN/m³)	15.65	17.10
Friction angle, ϕ (°)	36.40	41.00
Cohesion, c (kN/m²)	0.30	0.30
Dilatancy angle, ψ (°)	4.00	10.00
Secant stiffness, $E_{50}^{ref.}$ (kN/m²)	14600	28000
Unloading/reloading stiffness, $E_{ur}^{ref.}$ (kN/m²)	43800	72500
Oedometer stiffness, $E_{oed.}^{ref.}$ (kN/m²)	14600	28000
Unloading/reloading poission ratio, ν_{ur}	0.20	0.20
Reference stress for stiffness, $p^{ref.}$ (kN/m²)	100	100
Power, m	0.50	0.50
Failure ratio, R_f	0.90	0.90
The coeficient of lateral earth pressure at rest, K_0^{nc}	0.407	0.343

loading. $E_{ur}^{ref.}$ is used to model the elastic behavior in unloading and reloading and for many practical applications, it can be calculated by the equation of $E_{ur}^{ref.}$=3x$E_{50}^{ref.}$. The $E_{oed}^{ref.}$ is used to model plastic straining due to primary compression and it can be taken as $E_{oed.}^{ref.}$=$E_{50}^{ref.}$. The value of the failure ratio R_f is between 0.75-1.00 for most soils (ZSoil 2018). In Plaxis, a value of 0.9 is usually used for R_f as an average default value. The elastic unloading-reloading poisson's ratio is selected as 0.2 for most soils. In advanced soil models, loading history could be taken into account by using overconsolidation ratio (OCR) or pre-overburden pressure (POP). K_0 coefficient calculated by $K_{0\text{-}procedure}$ is a stress-dependent value and affected from the $K_{0\text{-}nc}$, ν_{ur}, OCR and POP parameters. The value of K_0 coefficient should be arranged using OCR or POP in overconsolidated soils. In validation analyses, load-settlement curves obtained for different POP values were compared to experimental load-settlement curves and suitable POP value was selected to account for the lightly overconsolidated state of sand. On the other hand, for normally consolidated state assumed in the analyses performed in layered conditions, the initial stresses were generated by $K_{0\text{-}procedure}$ considering as OCR=1 and POP=0.

The value of K_0 coefficient was calculated by Jaky's empirical equation, $K_0^{nc}=1-\sin\phi'$. Dilatancy angles were estimated by the following equation proposed by Bolton (1986) using the laboratory test results. Peak dilatancy angle can be calculated from ψ_{peak}=3.75I_R under triaxial conditions for $0<I_R<4$. I_R, I_D and p' can be defined as relative dilatancy index, relative density and mean effective stress at failure, respectively.

$$I_R = I_D\,(10 - \ln p') - 1 \quad (1)$$

Plaxis offers three different options to model the undrained behaviour of clay soil such as Undrained (A), Undrained (B) and Undrained (C). Since the soil behaviour is governed by effective stresses, Undrained (A) method is preferred to model the undrained behaviour of clay soil. But, in this case, the development of the pore pressure plays an important role in providing the right effective stress path that leads to failure at a realistic value of undrained shear strength. However, the right effective stress path in undrained loading can not be provided in most soil models.

As a result, these soil models will produce the wrong undrained shear strength if the material strength has been specified on the basis of effective strength parameters. It is so difficult to obtain accurate and reliable test results related to the effective shear strength parameters in projects on soft soils. Although the field and laboratory tests often carried out under undrained conditions it is not easy to determine the effective shear strength parameters through the experimental results obtained undrained conditions. The experimentally measured undrained Young's modulus can be converted into effective Young's modulus based on Hooke's law. But the advanced soil models do not include such a direct conversion. In Undrained (B) option, a direct control can be achieved on shear strength since undrained shear strength value is directly specified as an input parameter. Undrained effective stress analysis can be performed setting the $\phi=\phi_u=0$, $c=s_u=c_u$ and using effective stiffness parameters (E' and ν'). The value of m coefficient is usually taken as equal to zero in the undrained behaviour of fine grained soils. When the HS model is used with Undrained (B) option, the stiffness moduli in the model are no longer stress-dependent and the model exhibits no compression hardening. In this case, a constant stiffness value is used as such in Mohr-Coulomb (MC) model. MC model is usually preferred in the cases where the number of soil tests and the parameter database are limited (Plaxis 3D 2012, Dustin 2013, ZSoil 2018). Therefore, undrained behavior of clay was modeled with Mohr-Coulomb (MC) material model using the Undrained (B) option. In order to ensure realistic analysis results, the bulk modulus of the water must be higher than the bulk modulus of the soil skeleton. This condition can be satisfied by taking $\nu'\leq 0.35$.

For elastic behavior of clay, the value of ν'=0.33 was selected and undrained Young's modulus was calculated by E_u=500xc_u. It was assumed that the deformation modulus and undrained shear strength of clay were constant throughout the depth. Poulos and Small (2000) stated that the E' modulus could be obtained by multiplying the E_u modulus with β correction coefficient. The β coefficient is suggested as 0.4 for soft clay and 0.6 for stiff clay. In this study, the β coefficient was selected 0.5 considering the different consistencies of clay.

Table 3 MC model parameters for clay soil in layered soil analyses

Parameter	
Friction angle, ϕ' (°)	$\phi' = \phi_u = 0°$
Undrained Shear Strength, c_u (kPa)	10, 20, 40, 60
Unit weight, γ_{clay} (kN/m^3)	21.00
Dilation angle, ψ (°)	0
Poisson's ratio, ν'	0.33

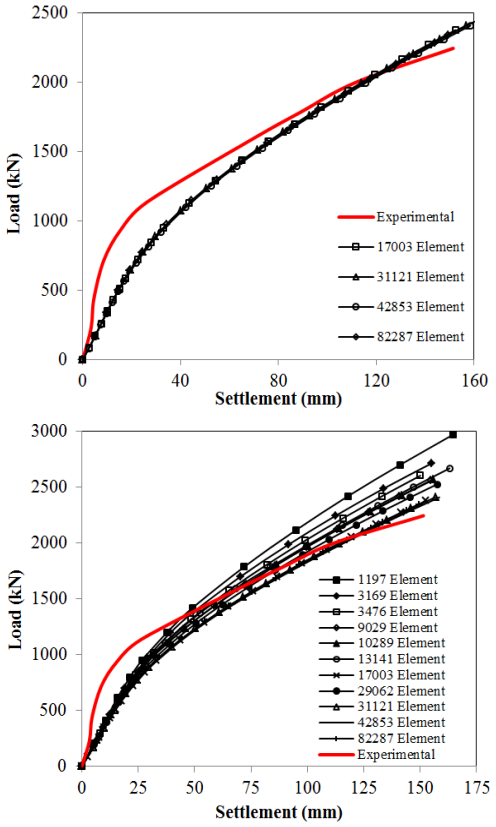

(a) The load-displacement curves obtained for different mesh densities

(b) Mesh densities which no further improvement observed

Fig. 1 Load-settlement curves obtained from the validation analyses performed to define the suitable mesh density

$$E' = \beta \, x \, E_u \tag{2}$$

Apart from heavily overconsolidated clay layers, dilatancy behavior is not seen in clays. Dilatancy angle is accepted as ψ=0 in clay soils. (Bowles 1997, Plaxis 3D 2012, Briaud 2013, Dustin 2013, ZSoil 2018, Amornfa *et al.* 2022). The properties of clay soil are summarized in Table 3.

In validation analyses, the square footing has been modelled using both non-porous volume element and plate element. It was assumed that footing behavior is linear elastic. The thickness of the footing has been chosen 76 cm as equal to that one used in the experimental studies. The footing was considered as very rigid and perfectly rough therefore the value of R_{inter} coefficient representing the interface behavior was selected as 1.0. Young's modulus, Poisson's ratio and unit weight for the footing were chosen as 32x10^6 kN/m^2, 0.2 and 24.0 kN/m^3, respectively. The load-settlement curves obtained from the analyses where the footing was modeled as non-porous volume element showed much better agreement with the experimental curves. Due to the symmetry existing both in x and y axes of the footing, only a quarter of the model geometry was employed to carry out the analyses. In layered soil analyses, footing thickness was selected as t=0.50 m and loading was applied as uniformly distributed pressure. Also, the depth of footing was equal to footing thickness. The validation analyses were performed for the 3.0 m x 3.0 m square footing on sand. To eliminate the boundary effect due to loading, the lateral distances were taken as the three times the footing width from the footing edge in both directions and the vertical distance was taken as the five times the width of footing from the footing base. Consequently, the dimensions of the model geometry were defined as 10.50 m x 10.50 m x 15.00 m. Plaxis generates full fixity at the base of the geometry whereas the vertical side boundaries were free vertically and constrained laterally. The Plaxis allows a fully automatic mesh generation considering the soil layers, structural members, boundary and loading conditions. The soil medium within the chosen domain was modelled using the 10-noded tetrahedral elements. Validation analyses have been performed with varying mesh densities to investigate the effect of mesh density on the results. Mesh was refined around the footing considering the different distances from the footing base and footing edges. The load-settlement curves obtained from a series of analyses performed at different mesh densities for a 3.0 m square footing were compared to the experimental load-settlement curve in Fig. 1.

In the analyses, the number of elements was changed from 1197 to 82287. As seen in Fig. 1, no significant changes were observed after a certain mesh density. At this point, the load-settlement curves overlap with each other and show good agreement with the experimental load-settlement curve. However, increasing mesh density requires longer computational time due to the large number of elements involved. Therefore, the mesh density yielding the closest results to the experimental one in the most convenient calculation time was selected. It was observed that average element sizes were compatible with each other for the analyses although there were minor differences in finite element number and node number depending on layering conditions, footing widths and the dimensions of the zone where mesh refined. Fig. 2 compares the load-settlement curves predicted by FE analyses with those measured in footing loading tests. As seen in Fig. 2, the load-settlement curves obtained from the FE analyses show good agreement with the experimental load-settlement curves. However, experimental load-settlement curves exhibit more stiff behaviour especially in the initial parts of the curves compared to load-settlement curves obtained from FE analyses. The differences between the initial parts of the curves may be attributed to the underestimation of the

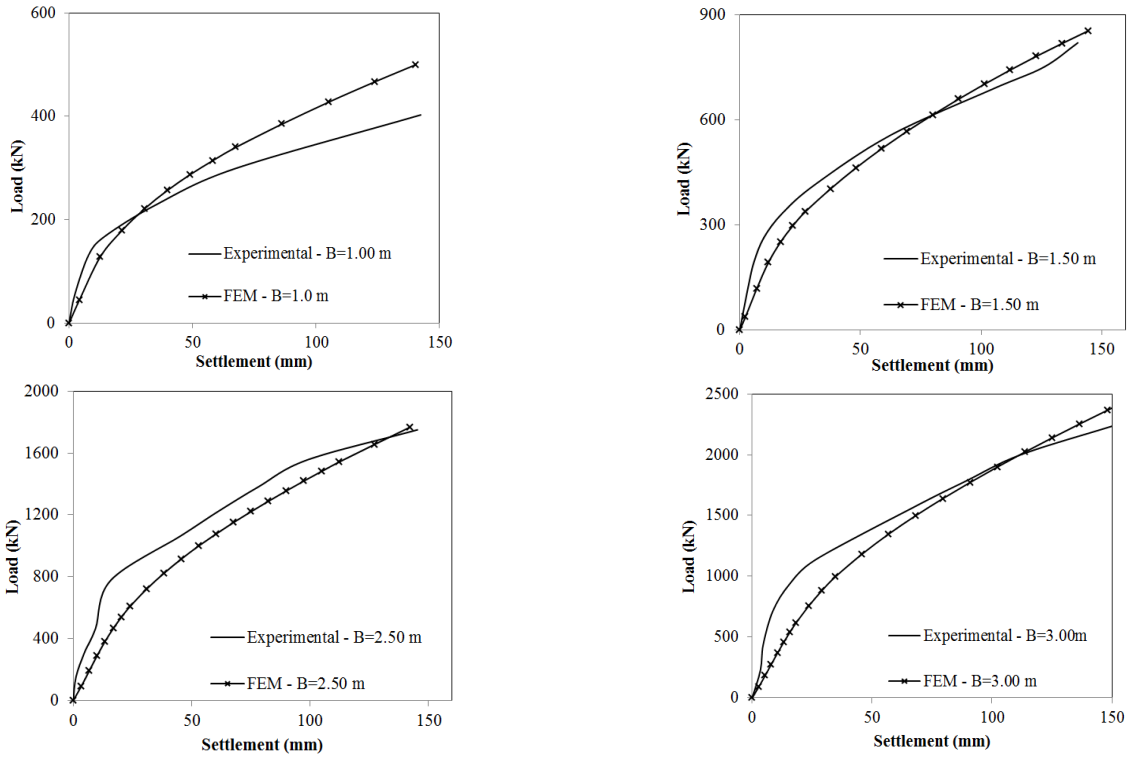

Fig. 2 Comparison of measured and predicted load-settlement curves

preconsolidation pressure in the upper part of subsoil depending on the disturbance effects.

3. Multigene genetic programming

Genetic programming (GP) is a symbolic optimization technique that uses Darwinian natural selection principle (Koza and Poli 2005). And also, GP is an extension of the Genetic Algorithm (GA) and is also called tree-based GP. At the end of the 1980s, GP developed further on the symbolic regression studies using a tree population (Koza 1992). One of them is Multigene Genetic Programming (MGGP) introduced by Searson *et al.* (2007) which is a robust version of GP. MGGP creates one or more traditional GP trees for each individual. These trees might all be thought of as "genes". The output of the MGGP model is obtained by a weighted linear combination of genes, and typically the MGGP model provides a mathematical expression for estimating an output variable using corresponding input variables as defined in Eq. (3).

$$y_p = f(X_1, X_2, \dots, X_N) \quad (3)$$

Where y_p shows the output response, f shows the symbolic nonlinear function or collection of nonlinear functions and $X_1, X_2, \dots, X_N$ shows input variables (N is number of input variable).

An illustration for the symbolic regression process in the MGGP model consisting of two genes and four inputs is shown in Fig. 3(a). Here, y_p represents the model output, x_1, x_2, x_3 and x_4 are the input variables, c_0 is the bias, b_1 and b_2 are the weight variables. Crossover and mutation operations are two major genetic recombination processes in MGGP. An illustration for the crossover operation is shown in Fig. 3(b). The crossover operation is performed for obtaining of a new child tree by exchanging randomly selected sub-trees over the two parent trees. The mutation process is performed on a single parent tree and is shown in Fig. 3(c). (Golap *et al.* 2021). Although the impressive modeling and prediction skill, MGGP method has not found much usage in solving the civil engineering problems.

4. Multigene genetic programming application

Authors tried to develop a model to estimate the reliable ultimate bearing capacity value based on the physical and strength properties of soil layers which can be easily quantified by any conventional laboratory and field tests together with geometrical dimensions in the problem considered. The main objective of this paper is to propose a bearing capacity equation for square footings resting on a strong sand layer overlying a weak clay layer using the MGGP modelling which is a machine learning technique. An extensive data set that represents the problem well enough is needed to do this. But it is so difficult to create a data set having these features due to the rarity of loading tests in prototype scale performed in the field, the few in number of laboratory model tests, inconsistencies between the test conditions, disadvantages of the laboratory model tests etc. Therefore, the data used in MGGP modelling was produced by FE analyses. However, parametric values used for material models in FE analyses should be realistic values obtained experimentally. This condition limits the number of data and scenarios to be evaluated especially in terms of the soil layers.

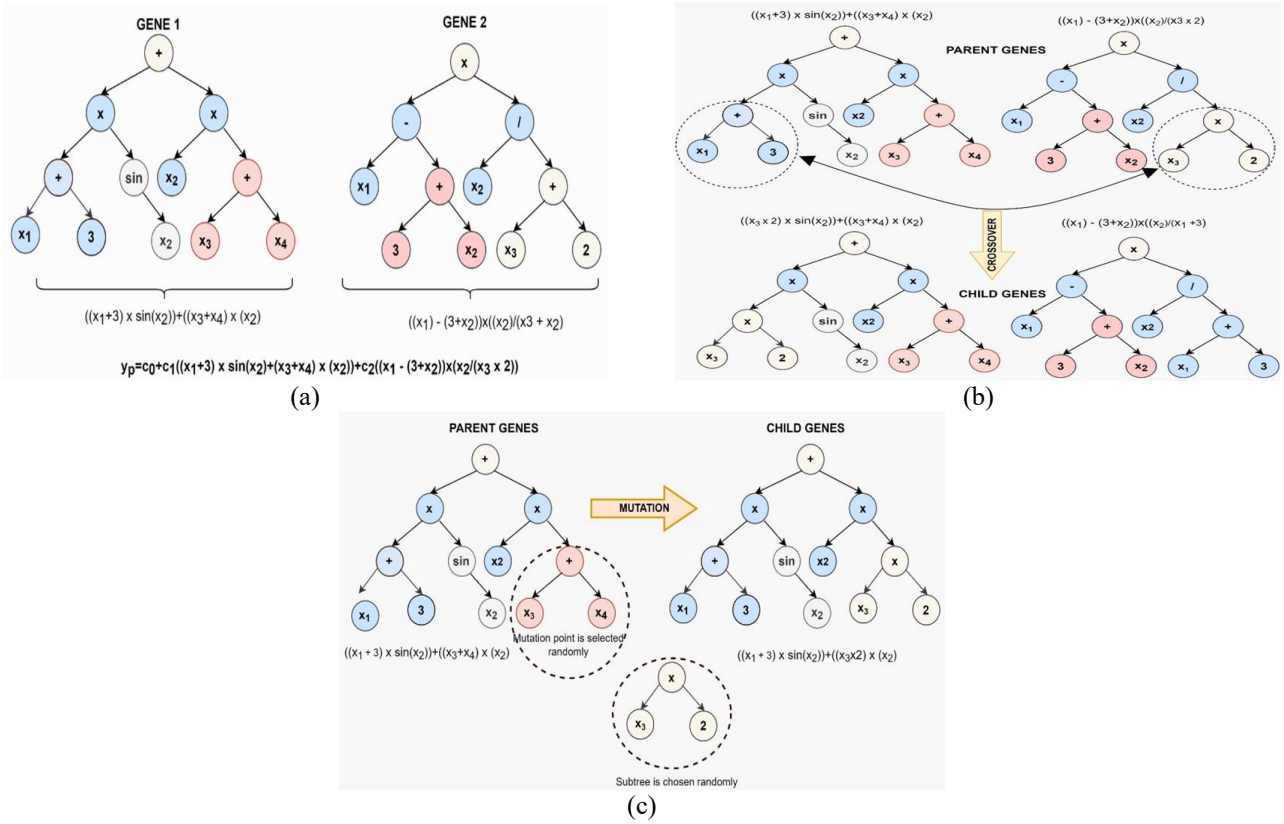

Fig. 3 An illustration for (a) tree structure of symbolic regression model, (b) crossover operation and (c) mutation operation

In the FE analyses carried out to produce the data, considered values of H/B ranged from 0.50 to 3.00. Since the homogeneous sand condition is an upper limit for the bearing capacity of layered soil, this condition was also evaluated in the analyses. The values of the undrained shear strength for weak clay layer were chosen as 10, 20, 40 and 60 kPa considering the different consistencies of clay such as very soft, soft, medium and stiff that might be expected in practice (BSI Standards Publication 2015). The FE analyses have been conducted for three different footing widths of 1.0 m, 2.0 m and 3.0 m. Two values of friction angle were adopted as 36.4° and 41° for the sand in FE analyses. These values were thought to be appropriate to model the medium-dense and dense sand conditions, respectively. It is well known that the effective internal friction angle, ϕ' is a stress dependent parameter and has significant effects on the bearing capacity, load-settlement behavior and development of failure mechanism in layered soil condition. In the analytical methods used to estimate the bearing capacity of layered soils, the shearing resistance arising from punching effect along the side surfaces of the sand block between the base of the footing and the surface of clay layer is taken into account by K coefficient. Although the chosen value of lateral earth pressure coefficient (K) can have an important influence on the calculated bearing capacity there is not a consensus on how its value should be defined. Every method has its own K coefficient assumption. K coefficient can take a value between the values of the active lateral earth pressure coefficient, K_a and passive lateral earth pressure coefficient, K_p or can be equal to K_0 or K_p. On the other hand, Meyerhof (1974) and Hanna and Meyerhof (1980) use the punching shear coefficient defined through the chart developed by the authors while Okamura *et al.* (1998) uses the K_p coefficient for this purpose. In this study, K_E coefficient obtained following the items defined below was used as an input parameter to consider the effect of ϕ' on the bearing capacity behavior of layered soils.

- The average vertical effective stress was calculated in the upper sand layer of H thickness by the expression that $\sigma'_{v\text{-}average} = (\gamma'_{sand} \, x \, H) / 2$.
- The K_E coefficient was obtained as the mean value of the K_a and K_p coefficients, $K_E=(K_a+K_p)/2$.
- Lateral effective stress was calculated by the equation that $\sigma'_h = \sigma'_{v\text{-}average} \, x \, K_E$.
- The σ'_h was multiplied by friction coefficient, $tan\phi'$ and then divided by the atmospheric pressure P_a, to obtain the normalized normal pressure, $P_E = (\sigma'_h \, x \, tan\phi') / P_a$.

Unit weight of the sands used for the medium-dense and dense conditions were γ=15.65 kN/m³ and 17.10 kN/m³, respectively. Since it was assumed that clay layer exhibited undrained behavior, obtained bearing capacity values are independent of clay unit weight (Michalowski and Shi 1995, Merifield *et al.* 1999, Shiau *et al.* 2003). There are different approaches in the literature for defining the ultimate bearing capacity from load-settlement curves. One of them is the 0.1B method proposed by Briaud and JeanJean (1994). According to this approach, the load value

Table 4 Statistical parameters of input and output variables

Statistical parameters	B (m)	H/B	c_u (kN/m²)	γ_{sand} (kN/m³)	P_E	$q_{u\text{-}s/B=0.1}$ (kN/m²)
Mean	2.00	2.55	32.50	16.38	0.72	835.19
SD	0.82	3.03	19.25	0.73	0.72	486.55
C_v (%)	40.93	118.91	59.24	4.44	99.62	58.26
C_s	-1.51	9.57	-1.43	-2.02	2.12	0.14
C_k	0	3.04	0.28	0	1.67	1.00
Max.	3.00	15.00	60.00	17.10	2.80	2094.41
Min.	1.00	0.50	10.00	15.65	0.06	160.11
Medyan	2.00	1.75	30.00	16.38	0.44	677.67
Mod	1.00	0.50	10.00	15.65	0.18	560.90

C_v: Coefficient of variation, *SD*: Standard deviation, C_s: Coefficient of skewness, C_k: Coefficient of kurtosis

resulting in settlement of 10% of the footing width is accepted as the failure load (Vesic 1973, Amar *et al.* 1994, Briaud and Jeanjean 1994, Lutenegger and Adams 1998, Cerato 2005, Cerato and Lutenegger 2007, Lavasan and Ghazavi 2012). In this study, the ultimate bearing capacity, q_u, was defined as the failure load or the unit load, $q_{u\text{-}s/B=0.1}$, causing a displacement equal to 10% of the footing width under the footing center.

An extensive data set covering the problems that can be encountered frequently in practice (with respect to the parametric value ranges) has been used. The ranges of the parameters also show good agreement with the study of Okamura *et al.* (1998). A total of 192 3D FE analyses have been performed to create a data set for MGGP modelling. The problem was modeled by 5 input and 1 output parameters using the GPTIPS toolbox written in MATLAB (Searson *et al.* 2010). Input parameters used in the model study include the width of the footing (B), the ratio of the thickness of upper sand layer to the footing width (H/B), undrained shear strength of lower clay (c_u), unit weight of upper sand layer (γ) and normalized normal stress (P_E). The failure load or the unit load causing a settlement of 10% of the footing width ($q_{u\text{-}s/B=0.1}$) was estimated as the output value.

Before to perform modeling with MGGP method, definitive statistics of the data were evaluated and resulting findings are summarized in Table 4.

As can be seen from Table 4, the kurtosis coefficients (C_k) belonging to the H/B, c_u, P_E and $q_{u\text{-}s/B=0.1}$ parameters are greater than zero and exhibit platokurtic distribution. Since skewness coefficients (C_s) for the H/B, P_E and $q_{u\text{-}s/B=0.1}$ parameters are greater than zero, they show a right skewed (positive skewness) distribution. On the other hand, the C_s coefficient of the B, c_u and γ_{sand} parameters are smaller than zero and the distribution of them is left skewed. The probability density function of the H/B parameter is the most variable due to the highest value of the C_v coefficient. γ_{sand} parameter which has the smallest C_v coefficient exhibits homogeneous distribution around the arithmetic mean. In other words, γ_{sand} parameter has the least variable property compared to other parameters.

The available data set which consists of total 192 data was divided into three data subsets as training, testing and validation. The number of the data in the training, testing and validation data sets were the 68%, 16% and %16 of the total data, respectively. The data subsets with specified numbers were created selecting the data randomly from total data for each of the trial. Determining the values of the appropriate control parameters before construction of the model is an important issue that affects the realization capability of the model. Model complexity directly depends on the number of correct populations, maximum tree depth, and number of generations. The control parameters applied for the modeling of the $q_{u\text{-}s/B=0.1}$ data in this study are shown in Table 5. These parameters were obtained by trial and error and after several preparatory studies.

Table 5 Control parameters for MGGP

Parameter	Value
Population Size	100
Fitness function	Mean square error
Maximum Generation	2000
Function Set	+,-,x, square, log, exp, power, rdvide
Maximum tree depth	6
Number of gene	6
Probability of Crossover	0.85
Probability of Mutation	0.10

Before the modeling study, random permutation was performed to prevent overfitting. The validation data set was used for the parameter calibration during the determination of hyper parameters of MGGP model trained by training data. The performance of the MGGP model of which parameters were defined with respect to the performance of validation data set was tried on the testing data set. Five random trials were performed in this way. The final model was determined according to the best result in the test stage comparing the performance criteria obtained in the training and testing phases. The flow chart of the study is shown in Fig. 4.

The Mean Absolute Error (MAE), Mean Square Error (MSE), Correlation Coefficient (R), and Determination Coefficient (R^2) metrics are used to evaluate the performance of the suggested model. Table 6 lists the formulae for the performance metrics that are utilized. The degree, direction, and significance of the relationship between the modeled and produced data are displayed by the correlation coefficient. The coefficient of determination

Table 6 Performance evaluation parameters used in this study

Metric	Description	Formula
MAE	Mean Absolute Error	$MAE = \frac{1}{N}\sum_{i=1}^{N}\lvert X_{produced,i} - X_{modeled,i}\rvert$
MSE	Mean Square Error	$MSE = \frac{1}{N}\sum_{i=1}^{N}(X_{produced,i} - X_{modeled,i})^2$
R	Correlation Coefficient	$R = \frac{1}{N-1}\sum_{i=1}^{N}\left(\frac{X_{produced,i} - \mu_X}{\sigma_X}\right)\left(\frac{X_{modeled,i} - \mu_{Xmodeled}}{\sigma_{Xmodeled}}\right)$
R^2	Determination Coefficient	$R^2 = 1 - \frac{\sum_{i=1}^{N}[X_{produced,i} - X_{modeled,i}]^2}{\sum_{i=1}^{N}[X_{produced,i} - \mu_X]^2}$

Table 7 Performance criteria for training and testing stages of five random trials

Random Trials		MSE	MAE	R	R^2
1	Train	5.4307762e+03	5.7783719e+01	9.8828298e-01	9.7670325e-01
	Test	1.1143628e+04	8.1419459e+01	9.6641787e-01	9.3396350e-01
2	Train	6.1128839e+03	6.0557811e+01	9.8529964e-01	9.7081538e-01
	Test	6.8924523e+03	6.7719280e+01	9.9044126e-01	9.8097389e-01
3	**Train**	**1.9446018e+03**	**3.5297166e+01**	**9.9552794e-01**	**9.9107588e-01**
	Test	**2.7138745e+03**	**3.9606714e+01**	**9.9609811e-01**	**9.9221144e-01**
4	Train	4.9583867e+03	5.9082424e+01	9.8732868e-01	9.7481791e-01
	Test	6.8337381e+03	6.9040452e+01	9.8993934e-01	9.7997990e-01
5	Train	3.6130520e+03	4.6197348e+01	9.9267814e-01	9.8540988e-01
	Test	6.3448990e+03	5.7736029e+01	9.8899279e-01	9.7810673e-01
Whole Data		**2.2391030e+03**	**3.7604002e+01**	**1.0000000e+00**	**9.9050500e-01**

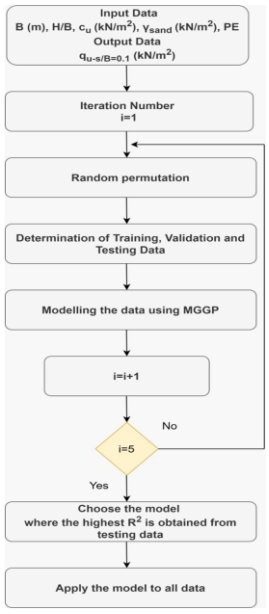

Fig. 4 Flow chart for application of the model

is the proportion of the variance of the dependent variable that can be predicted from the independent variables. It demonstrates that when the R^2 value gets closer to 1, the modeled and produced data become more correlated. The results obtained for each of the trials were demonstrated in Fig. 5. It is seen that the best results considering the performance criteria were obtained for the third random trial in both training and testing data sets. Therefore, the equation proposed in the third random trial was chosen to predict the ultimate bearing capacity and was applied whole data set. The comparison of the modeled and produced data for whole data set was showed in Fig. 6. The performance values of each random trial have been summarized in Table 7.

The most successful results have been obtained for the third random trial. The ultimate bearing capacity values calculated using the equation obtained in the third trial show fairly good agreement those of obtained from FE analyses. The results show that the R^2 values obtained for both training and testing stages are greater than 0.99. The other performance criteria also have the smallest values in this trial for both training and testing. The R^2 value between the modelled and produced data was obtained as 0.99 when the formula obtained in the third trial is applied the whole data.

5. Comparison of MGGP model results with existing formulae

The ultimate bearing capacity values estimated from the proposed equation have been compared to the bearing capacities calculated using the experimental methods

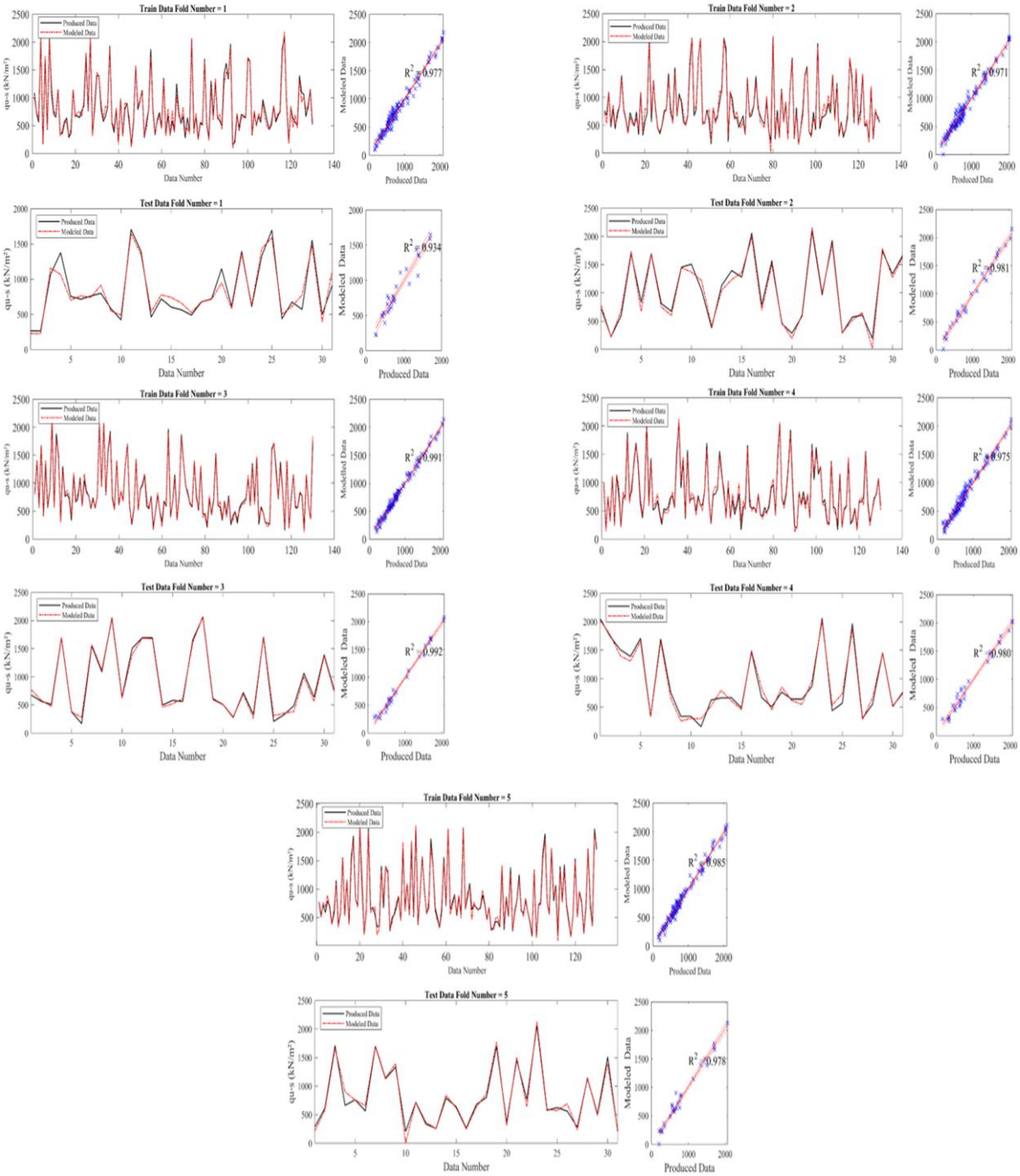

Fig. 5 Scatter-comparison graphs for modeled and produced q_u values in training and testing datasets

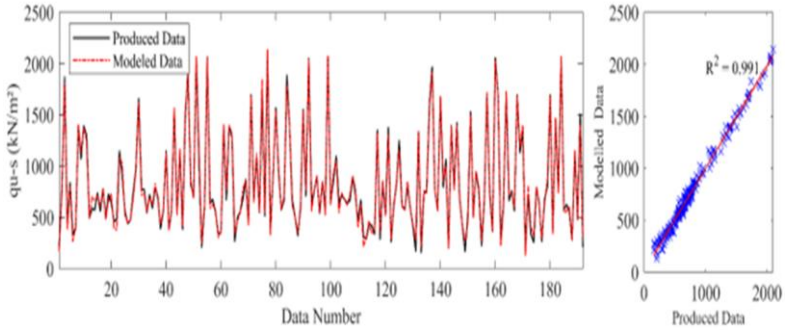

Fig. 6 The comparison of the modeled and produced data for whole data set

proposed by Meyerhof (1974) and Hanna and Meyerhof (1980) and Okamura *et al.* (1998) to evaluate the suitability of the formula.

The calculated ultimate bearing capacities using the semi-empirical analytical methods are different from each other because of the assumptions made in the methods are not the same. The shape of the sand block and description of shearing resistance acting along the side of the block are the most significant parameters affecting the bearing capacity values obtained. In PSM proposed by Meyerhof (1974) and Hanna and Meyerhof (1980) it is assumed that the ultimate bearing capacity of upper sand layer is much more than that of the underlying clay layer. Because the bearing capacity obtained in the cases of where both layers have similar individual bearing capacities will not be represent completely the bearing capacity of layered condition. At the time of failure deformation of the sand layer is less than that of the clay layer since the simultaneous occurrence of the failure in both layers will not be take place. The vertical displacement of sand column is much more than that of the lateral movements due to the weak clay layer. This lateral movement is not sufficient for the maximum mobilization of the passive pressure acting on the assumed vertical planes. Therefore, the mobilized angle of friction in the sand layer could be less than the peak value and shearing resistance along the side of the sand block is taken into account using the punching shear coefficient K_s. In this method, K_s is given in charts as a function of the friction angle of sand layer (ϕ_1) and the ratio of the bearing capacity of uniform clay to that of uniform sand (q_2/q_1). It is assumed that K_s coefficient is independent of footing depth. Hanna and Meyerhof (1980) proposed the following equations for ultimate bearing capacity of rectangular footings resting on a strong sand layer overlying saturated weak clay ($\phi_2=0$) layer. The smaller of the q_u and q_t values is chosen as the ultimate bearing capacity. q_u and q_t are defined as ultimate bearing capacity in layered state and ultimate bearing capacity of upper sand layer, respectively.

$$q_u = 5.14c_2\left[1+0.2\left(\frac{B}{L}\right)\right]+\left(1+\frac{B}{L}\right)\gamma_1 H^2\left(1+\frac{2D_f}{H}\right)\left(\frac{K_s tan\emptyset_1}{B}\right)\lambda_s + \gamma_1 D_f \le q_t \quad (4)$$

$$q_t = \gamma_1 D_f N_{q(1)}\left[1+0.1\left(\frac{B}{L}\right)tan^2\left(45+\frac{\emptyset_1}{2}\right)\right] + \frac{1}{2}\gamma_1 B N_{\gamma(1)}\left[1+0.1\left(\frac{B}{L}\right)tan^2\left(45+\frac{\emptyset_1}{2}\right)\right] \quad (5)$$

Both load spreading angle in the sand layer and shearing resistance along the side of the block are considered in the calculations proposed by Okamura *et al.* (1998). It is assumed that load spreading angle changes depending on the strength parameters of both layers and *H/B* ratio. The normal stress acting on the side of the sand block is equal to the K_p times the vertical stress. In the centrifuge tests conducted by Okamura *et al.* (1998), it was observed that the Rankine's passive coefficient K_p is a lower limit. Also, the horizontal stress on the side of the sand block was affected from both the strength of lower clay layer and depth of footing. In this method, the angle of shearing resistance mobilized on the side surfaces of the sand block is adopted as equal to ϕ'. Okamura *et al.* (1998) yields the following formulae for ultimate bearing capacity of a circular footing on a sand layer overlying clay layer.

$$q_f = \left(1+2\frac{H}{B}tan\alpha_c\right)^2(c_u N_c s_c + p_0' + \gamma' H) + \frac{4K_p sin(\phi'-\alpha_c)}{cos\phi' cos\alpha_c}\left\{\left(p_0' + \frac{\gamma' H}{2}\right)\frac{H}{B} + p_0' tan\alpha_c\left(\frac{H}{B}\right)^2 + \frac{2}{3}\gamma' H tan\alpha_c\left(\frac{H}{B}\right)^2\right\} - \frac{\gamma' H}{3}\left\{4\left(\frac{H}{B}\right)^2 tan^2\alpha_c + 6\frac{H}{B}tan\alpha_c + 3\right\} \quad (6)$$

The data produced by FE analyses carried out on prototype scale footings were modeled by MGGP method and then a bearing capacity equation given below was obtained.

$$q_u=(5.1e+15*x4*x5*(x4-1.8)*(x4+x5)^2)/((2.9e+17*(x4+5.0))/x3^(1.0*x2)+4.1e+17)-160.0*exp(x5)-63.0*log((x2*x5^x1*x5^2)/(x3*(x1+x4)))-4.7*(-1.6)^x1-4.7*x3*x5- 160.0*x2* exp(-1.0*x5)-(19.0*x1)/x5-4.7*x4*(x2-1.0*x3)-(3.3e+14*x5)/(7.0e+13*x5^x1- 2.0e+14)-(160.0*log(x2)^x1)/(log(x4-1.0*x2)*(x1+x5))-68.0*x3+(5.5e+15*x4*log(x2)*(x4-5.0)* (x4-5.9)*(x1+x4-(1.0*(x3-1.0*x4))/(x3+x4)))/(7.0e+17/x3^(1.0*x2)+3.6e+17)-(0.075*x5^x1*x5^2*log(x5)*(x1-1.0*x4)^2*(x2-2.0*x1+x4)*(2.0*x1-1.0*x4+4.9))/x2^4+ 73.0 \quad (7)$$

In this equation, *x1*, *x2*, *x3*, *x4* and *x5* variables represent the *B*, *H/B*, c_u, γ_{sand} and P_E parameters, respectively.

The reliability of the proposed equation was tried by a data set consisting of 20 data independent of the total data set used in MGGP modelling. These data are shown in Table 8.

The ultimate bearing capacity values obtained from the proposed equation for 20 independent data were compared to the ultimate bearing capacity values calculated using the semi-empirical analytical approaches proposed by Meyerhof (1974) and Hanna and Meyerhof (1980) and Okamura *et al.* (1998). The comparison of the results is demonstrated in Fig. 7. It can be seen from Fig. 7 that the bearing capacity values obtained from MGGP and PSM show a similar pattern. Although the ultimate bearing capacity values predicted using the formula produced by MGGP model are in good agreement with those calculated using the PSM, they are less than the values calculated by OM. The highest bearing capacities for all the 20 data have been obtained from the OM. The bearing capacity values estimated by MGGP are either a value between the bearing capacity values calculated using these two methods or the lowest bearing capacity value. This result indicates that the proposed equation yields the bearing capacity values which are on the safe side for all the data.

The Absolute Percentage Errors (APE) between the PSM and OM, MGGP and PSM and MGGP and OM have been calculated. The results are illustrated in Fig. 8. It is observed that the APE between the bearing capacities calculated using PSM and OM vary between the 26% and 155%. On the other hand, while the APE varies between 4% and 48% for the bearing capacities obtained from PSM and MGGP this range is equal to 3%-59% for those obtained

Table 8 The independent data set used to confirm reliability of the proposed bearing capacity equation

B (m)	H/B	c_u (kN/m²)	γ_{sand} (kN/m³)	P_E
2.80	0.75	27	15.65	0.253
1.75	1.00	33	15.65	0.211
2.25	1.40	17	15.65	0.379
1.50	0.50	22	15.65	0.090
1.60	1.25	33	15.65	0.241
2.10	1.35	37	15.65	0.341
2.60	1.80	15	15.65	0.564
1.20	1.00	25	17.10	0.224
1.70	0.85	51	17.10	0.270
2.35	1.40	23	17.10	0.614
2.40	0.70	13	17.10	0.314
1.65	0.80	36	17.10	0.246
2.30	0.90	16	15.65	0.249
1.40	1.50	52	15.65	0.253
2.90	1.35	22	15.65	0.471
1.90	0.30	31	17.10	0.106
2.10	0.40	34	15.65	0.101
2.20	0.85	12	15.65	0.225
1.35	1.60	43	17.10	0.403
2.55	1.10	17	17.10	0.524

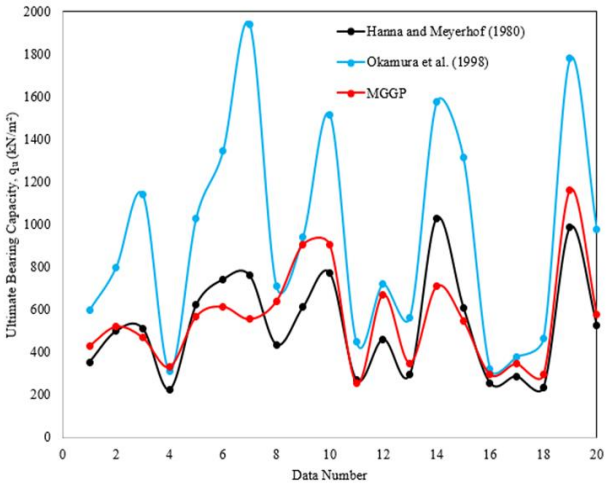

Fig. 7 The comparison of the ultimate bearing capacity values

from MGGP and OM. When the absolute percentage difference values of each of the 20 data are analyzed, it is observed that the differences in bearing capacities among the approaches considered do not change systematically depending on the input parameters used in MGGP modelling. In data where the differences between the bearing capacities obtained from the MGGP and PSM are least, the difference values between the MGGP and OM are usually high. The similar situation is valid for the comparison between the MGGP and OM. Such that, in data where the differences between the bearing capacities obtained from the MGGP and OM are least, the difference values between the MGGP and PSM are also usually high.

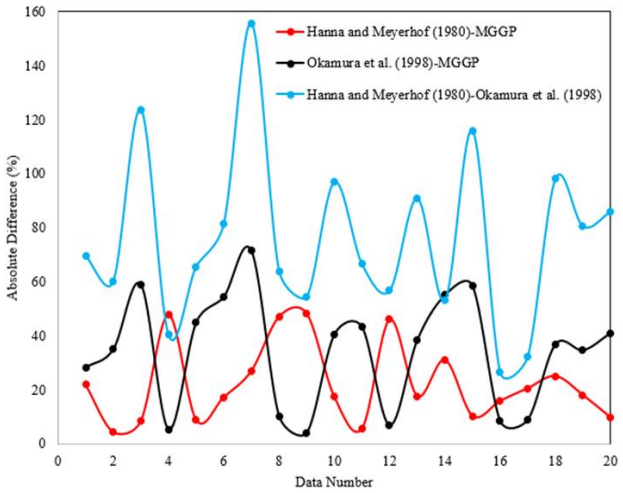

Fig. 8 The comparison of the absolute percentage error values

When the differences among the bearing capacity values obtained from three different method for all the 20 data have been compared, it is seen that the utmost differences are between the bearing capacity values calculated using the PSM and OM. This result also shows that the proposed formulation can model the problem accurately and reliably.

Although constant values of lateral earth pressure coefficient (K_E and K_P) depending on the ϕ' have been used in both the formulation proposed in this study and OM, K_s coefficient which varies depending on both ϕ' and q_2/q_1 is used in PSM. The results reveal that the assumptions made in the determination of K coefficient alone do not have a significant effect on the differences among the bearing capacities obtained from the methods considered.

Such that, the least PAE is equal to 4.172% between the bearing capacities obtained from PSM and MGGP. In this data, the values of K coefficients are equal to 3.813 and 2.087 for the PSM and MGGP, respectively. For the same data, the PAE is equal to 34.895% between the bearing capacities obtained from OM and MGGP while the value of K coefficient is 3.919 for OM. Similar results are valid also for the data in which the least PAE is obtained between the OM and MGGP methods. The PAE is equal to 3.870% for this data while the values of K coefficients are 4.815 and 2.511 for the OM and MGGP methods, respectively. For the same data, the PAE is equal to 48.273% between the bearing capacities obtained from PSM and MGGP while the value of K coefficient is 2.714 for PSM. The minimum value of PAE between the PSM and OM is 26.416% and the K coefficients are 3.250 and 4.815 for PSM and OM, respectively. On the other hand, the maximum PAE value is 155.625% between the PSM and OM while the values of K coefficients are 2.357 and 3.919 for the PSM and OM, respectively.

Although the value ranges of input parameters in whole data set are more compatible with the ranges of parameters in Okamura et al.'s experimental study the predicted bearing capacity values using the MGGP formula show much better agreement with the bearing capacities calculated with PSM.

6. Conclusions

In this study, authors used a hybrid approach including FEM and ML technique to develop an equation estimating the ultimate bearing capacity of a square footing on a sand layer overlying clay. The proposed equation is based on the physical and strength properties of soil layers which can be easily quantified by any conventional laboratory and field tests together with geometrical dimensions in the problem considered. Also, it does not require the use of any charts or calculations of different parameters. The results obtained in this study can be summarized as follows:

- The results indicate that the proposed equation yields the bearing capacity values which are on the safe side for all the data.
- It is observed that the differences in bearing capacities among the approaches considered do not change systematically depending on the input parameters used in MGGP modelling.
- It is seen that the utmost differences are between the bearing capacity values calculated using the PSM and OM.
- The results reveal that the assumptions made in the determination of K coefficient alone do not have a significant effect on the differences among the bearing capacities obtained from the methods considered.
- Although the value ranges of input parameters in whole data set are more compatible with the ranges of parameters in Okamura *et al.*'s experimental study the predicted bearing capacity values using the MGGP formula show much better agreement with the bearing capacities calculated with PSM.
- It was observed that the MGGP method yielded successful results for the problem considered. The proposed equation provides reasonable predictions and efficient enough to be used in practice.

Since AI techniques are data-driven, performance of the models significantly depends on the data provided to make predictions. In this study, data produced through numerical modelling have been used. Numerical data are very useful when there are not enough experimental data or when obtaining experimental data are difficult and expensive. The number of data used for AI model training is one of the most important factor affecting the accuracy of the model. Generally, the use of larger dataset will result in better performance of the AI techniques. Data selection for data subsets (e.g., training, testing and validation) and distribution ratio between the three subsets may also have substantial effects on model performance. The developed AI models are applicable to problems with similar properties, but care should be taken when applying them to scenarios with different properties because extrapolation is required for new data outside the range of the trainig data (Jong *et al.* 2021, Baghbani *et al.* 2022, Onyelowe *et al.* 2023). Despite of these limitations, the results of this study prove that the proposed equation can be used reliably for the value ranges of the parameters in the data set. If a much larger data set including sand and clay soils with different properties, different footing sizes and footing depths, different layered scenarios etc. is created a more robust bearing capacity equation can be produced through the methodology used in this study.

Formatting of funding sources

This research did not receive any specific grant from funding agencies in the public, commercial, or not-for-profit sectors.

CRediT authorship contribution statement

Erdal Uncuoğlu: Conceptualization, Methodology, Formal Analysis, Investigation, Data Curation, Writing—review and editing, Data collection, Software, Validation. **Levent Latifoğlu:** Software, Validation, Data Curation, Original Draft Preparation. **Zulkuf Kaya:** Conceptualization, Software, Writing—review and editing, Original Draft Preparation.

Declaration of competing interest

The authors declare that they have no known competing financial interests or personal relationships that could have appeared to influence the work reported in this paper.

Data availability

Data will be made available on request.

References

Amar, S., Baguelin, F., Canepa, Y. and Frank, R. (1994), "Experimental study of the settlement of shallow foundations", *Geotechnical Special Publication, ASCE,* **40**(2), 1602-1610.

Amornfa, K., Quang, H.T. and Tuan, T.V. (2022), "3D numerical analysis of piled raft foundation for Ho Chi Minh City subsoil conditions", *Geomech. Eng.*, **29**(2), 183-192. https://doi.org/10.12989/gae.2022.29.2.183.

Arel, E. (2012), "Predicting the spatial distribution of soil profile in Adapazari/Turkey by artificial neural networks using CPT data", *Comput. Geosci.*, **43**, 90-100. https://doi.org/10.1016/j.cageo.2012.01.021.

Askari, M., Khalkhali, A.B., Makarchian, M. and Ganjian, N. (2021), "The bearing capacity of circular footings on sand with thin layer: An experimental study", *Geomech. Eng.*, **27**(2), 123-130. https://doi.org/10.12989/gae.2021.27.2.123.

Baghbani, A., Choudhury, T., Costa, S. and Reiner, J. (2022), "Application of artificial intelligence in geotechnical engineering: A state-of-the-art review", *Earth-Sci. Rev.*, **228**, 103991. https://doi.org/10.1016/j.earscirev.2022.103991..

Bhattacharya, B. and Solomatine, D.P. (2006), "Machine learning in soil classification", *Neural Networks*, **19**(2), 186-195. https://doi.org/10.1016/j.neunet.2006.01.005.

Bolton, M.D. (1986), "The strength and dilatancy of sands", *Geotechnique*, **36**(1), 65-78.

Bonini, N.A., Bonini, C.S.B., Bisi, B.S., Reis, A.R. and Coletta, L.F.S. (2017), "Artificial neural network for classification and analysis of degraded soils", *IEEE Latin Am. Transactions*, **15**(3), 503-509. https://doi.org/10.1109/TLA.2017.7867601.

Bowles, J.E. (1997), *Foundation Analysis and Design*, The McGraw-Hill Companies Inc., New York.

Briaud, J.L. and Jeanjean, P. (1994), "Load settlement curve method for spread footings on sand", *J. Geotech. Geoenviron.*

Eng., **133**(8), 905-920.
Briaud, J.L. and Gibbens, R. (1997), "Large-scale load tests and data base of spread footings on sand", Publication No. FHWA-Rd-97-068.
Briaud, J.L. (2013), *Geotechnical Engineering: Unsaturated and Saturated Soils*, John Wiley & Sons, Inc. Hoboken, New Jersey.
BSI Standards Publication (2015), "*Code of Practice for Foundations*", BS 8004:2015: The British Standards Institution.
Bui, D.T., Moayedi, H., Gör, M., Jaafari, A. and Foong, L.K. (2019), "Predicting slope stability failure through machine learning paradigms", *ISPRS Int. J. Geo-Information*, **8**(9), 395. https://doi.org/10.3390/ijgi8090395.
Carvalho, L.O. and Ribeiro, D.B. (2019), "Soil classification system from cone penetration test data applying distance-based machine learning algorithms", *Soils and Rocks*, **42**(2), 167-178. https://doi.org/10.28927/SR.422167.
Cerato, A.B. (2005), "Scale effect of shallow foundation bearing capacity on granular material", Ph.D. Dissertation, University of Massachusetts Amherts, MA, USA.
Cerato, A.B. and Lutenegger, A.J. (2007), "Scale effect of shallow foundation bearing capacity on granular material", *J. Geotech. Geoenviron. Eng.*, **133**(10), 1192-1202. https://doi.org/10.1061/(ASCE)10900241(2007)133:10(1192).
Dustin, R. (2013), "Initial elastic modulus degradation using pressuremeter and standard penetration test results at two sites", Master of Science Thesis, University of Nevada Las Vegas.
Eshkevari, S.S. (2018), "Bearing capacity of surface strip footings on layered soils", Ph.D. Dissertation, The University of Newcastle, Australia.
Eshkevari, S.S., Abbo, A.J. and Kouretzis, G. (2019), "Bearing capacity of strip footings on sand over clay", *Can. Geotech. J.*, **56**, 699-709. https://doi.org/10.1139/cgj-2017-0489.
Ferentinou, M.D. and Sakellariou, M.G. (2007), "Computational intelligence tools for the prediction of slope performance", *Comput. Geotech.,* **34**(5), 362-384. https://doi.org/10.1016/j.compgeo.2007.06.004.
Goh, A.T.C. and Goh, S.H. (2007), "Support vector machines: their use in geotechnical engineering as illustrated using seismic liquefaction data", *Comput. Geotech.*, **34**(5), 410-421. https://doi.org/10.1016/j.compgeo.2007.06.001.
Golap, M.A.U., Raju, S.T.U., Haque, M.R. and Hashem, M.M.A. (2021), "Hemoglobin and glucose level estimation from PPG characteristics features of fingertip video using MGGP-based model", *Biomed. Signal Pr. Control*, **67**, 102478. https://doi.org/10.1016/j.bspc.2021.102478.
Gomes, Y.F., Verri, F.A.N. and Ribeiro, D.B. (2021), "Use of machine learning techniques for predicting the bearing capacity of piles", *Soils Rocks*, **44**(4). https://doi.org/10.28927/SR.2021.074921.
Hanna, A.M. and Meyerhof, G.G. (1980), "Design charts for ultimate bearing capacity of foundations on sand overlying soft clay", *Can. Geotech. J.*, **17**, 300-303.
Hanna, A.M. (1981), "Foundations on strong sand overlying weak sand", *J. Geotech. Eng. Div.*, **107**(7), 915-927.
Hanna, A.M., Ural, D. and Saygili, G. (2007), "Neural network model for liquefaction potential in soil deposits using Turkey and Taiwan earthquake data", *Soil Dyn. Earthq. Eng.*, **27**(6), 521-540. https://doi.org/10.1016/J.SOILDYN.2006.11.001.
Jaky, J. (1944), "The coefficient of earth pressure at rest", *J. Soc. Hungarian Architect. Engineers*, 78, 355-358.
Jong, S.C., Ong, D.E.L. and Oh, E. (2021), "State-of-the-art review of geotechnical-driven artificial intelligence techniques in underground soil-structure interaction", *Tunn. Undergr. Sp. Tech.*, **113**, 103946. https://doi.org/10.1016/j.tust.2021.103946.
Juang, C.H. and Chen, C.J. (1999), "CPT-based liquefaction evaluation using artificial neural networks", *Comput. -Aided Civil Infrastruct. Eng.*, **14**(3), 221-229. https://doi.org/10.1111/0885-9507.00143.
Kohestani, V.R., Hassanlourad, M. and Ardakani, A. (2015), "Evaluation of liquefaction potential based on CPT data using random forest", *Nat. Hazards*, **79**(2), 1079-1089. https://doi.org/10.1007/s11069-015-1893-5.
Kovacevic, M., Bajat, B. and Gajic, B. (2010), "Soil type classification and estimation of soil properties using support vector machines", *Geoderma*, **154**(3-4), 340-347. https://doi.org/10.1016/j.geoderma.2009.11.005.
Koza, J.R. (1992), *Genetic Programming, on the Programming of Computers by Means of Natural Selection*, MIT Press, Cambridge.
Koza, J.R. and Poli, R. (2005), *Genetic Programming, in: Search Methodologies*, Springer, Boston, MA.
Laman, M. and Yildiz, A. (2007), "Numerical studies of ring foundations on geogrid reinforced sand", *Geosynthetics Int.*, **14**(2), 52-65. https://doi.org/10.1680/gein.2007.14.2.52.
Laman, M. and Uncuoglu, E. (2009), "Prediction of the moment capacity of pier foundations in clay using neural networks", *Kuwait J. Sci. Eng.*, **36**(1), 1-20.
Lavasan, A.A. and Ghazavi, M. (2012), "Behavior of closely spaced square and circular footings on reinforced sand", *Soils Found.*, **52**(1), 160-167. https://doi.org/10.1016/j.sandf.2012.01.006.
Livingston, G., Piantedosi, M., Kurup, P. and Sitharam, T.G. (2008), "An approximate method to estimate the bearing capacity of piles", *Geotechnical Earthquake Engineering and Soil Dynamics IV Congress Reston: American Society of Civil Engineers*, (Eds., X. Zeng, M.T. Manzari and D.R. Hiltunen), 1-10.
Lo Presti, D.C.F., Jamiolkowski, M., Pallara, O., Pisciotta, V. and Ture, S. (1995) "Stress dependence of sand stiffness", *Proceedings of the International Conferences on Recent Advances in Geotechnical Earthquake Engineering and Soil Dynamics*, 71-76. https://scholarsmine.mst.edu/icrageesd/03icrageesd/session01/16.
Lutenegger, A.J. and Adams, M.T. (1998), "Bearing capacity of footings on compacted sand", *International Conference on Case Histories in Geotechnical Engineering*, pp. 1216-1224. https://scholarsmine.mst.edu/icchge/4icchge/4icchge-session01/36.
Maeda, K. and Miura, K. (1999), "Confining stress dependency of mechanical properties of sands", *Soils and Foundations*, 39, 53-67.
Maxwell, A.E., Sharma, M., Kite, J.S., Donaldson, K.A., Thompson, J.A., Bell, M.L. and Maynard, S.M. (2020), "Slope failure prediction using random forest machine learning and lidar in an eroded folded mountain belt", *Remote Sens.*, **12**(3), 486. https://doi.org/10.3390/rs12030486.
Merifield, R.S., Sloan, S.W. and Yu, H.S. (1999), "Rigorous plasticity solutions for the bearing capacity of two-layered clays", *Geotechnique*, **49**(4), 471-490. https://doi.org/10.1680/geot.1999.49.4.471.
Meyerhof, G.G. (1974), "Ultimate bearing capacity of footings on sand overlying clay", *Can. Geotech. J.*, **11**(2), 223-229.
Michalowski, R.L. and Shi, L. (1995), "Bearing capacity of footings over two-layer foundation soils", *J. Geotech. Eng.*, **121**(5), 421-428. https://doi.org/10.1061/(ASCE)0733-9410(1995)121:5(421).
Mosallanezhad, M. and Moayedi, H. (2017), "Comparison analysis of bearing capacity approaches for the strip footing on layered soils", *Arabian J. Sci. Eng.*, **42**, 3711-3722. https://doi.org/10.1007/s13369-017-2490-6.

Nejad, F.P., Jaksa, M.B., Kakhi, M. and McCabe, B.A. (2009), "Prediction of pile settlement using artificial neural networks based on standard penetration test data", *Comput. Geotech.*, **36**(7), 1125-1133. https://doi.org/10.1016/j.compgeo.2009.04.003.

Nejad, F.P. and Jaksa, M.B. (2017), "Load-settlement behavior modeling of single piles using artificial neural networks and CPT data", *Comput. Geotech*., **89**, 9-21. https://doi.org/10.1016/j.compgeo.2017.04.003.

Okamura, M., Takemura, J. and Kimura, T. (1998), "Bearing capacity predictions of sand overlying clay based on limit equilibrium methods", *Soils Found.*, **38**(1), 181-194.

Onyelowe, K.C., Mojtahedi, F.F., Ebid, A.M., Rezaei, A., Osinubi, K.J., Eberemu, A.O., Salahudeen, B., Gadzama, E.W., Rezazadeh, D., Jahangir, H., Yohanna, P., Onyia, M.E., Jalal, F.E., Iqbal, M., Ikpa, C., Obianyo, I.I. and Rehman, Z.U. (2023), "Selected AI optimization techniques and applications in geotechnical engineering", *Cogent Eng.*, **10**(1), 2153419. https://doi.org/10.1080/23311916.2022.2153419.

Pham, Q.N. and Ohtsuka, S. (2021), "Ultimate bearing capacity of rigid footing on two layered soils of Sand-Clay", *Int. J. Geomech.*, **21**(7), 04021115. https://doi.org/10.1061/(ASCE)GM.1943-5622.0002095.

Plaxis 3D (2012), Delft, Netherlands.

Poulos, H.G. and Small, J.C. (2000), *Development of Design Charts for Concrete Pavements and Industrial Ground Slabs, Chapter 2, Design Applications of Raft Foundations*, Hemsley, Thomas Telford.

Samui, P. (2008), "Support vector machine applied to settlement of shallow foundations on cohesionless soils", *Comput. Geotech.*, **35**(3), 419-427. https://doi.org/10.1016/j.compgeo.2007.06.014.

Sasmal, S.K. and Behera, R.N. (2021), "Application of artificial intelligence methods for predicting transient response of foundation", *Geomech. Eng.*, **27**(3), 197-211. https://doi.org/10.12989/gae.2021.27.3.197.

Searson, D.P., Willis, M.J. and Montague, G.A. (2007), "Co-evolution of nonlinear PLS model components", *J Chemometr*, 12, 592–603. https://doi.org/10.1002/cem.1084.

Searson, D.P., Leahy, D.E. and Willis, M.J. (2010), "Gptips: an open source genetic programming toolbox for multigene symbolic regression", *Proceedings of the International Multiconference of Engineers and Computer Scientists*, *IMECS*, Hong Kong.

Shiau, J.S., Lyamin, A.V. and Sloan, S.W. (2003), "Bearing capacity of a sand layer on clay by finite element limit analysis", *Can. Geotech. J.*, **40**, 900-915. https://doi.org/10.1139/t03-042.

Tang, C., Phoon, K.K., Zhang, L. And Li, D.Q. (2017), "Model uncertainty for predicting the bearing capacity of sand overlying clay", *Int. J. Geomech.*, **17**(7), 04017015. https://doi.org/10.1061/(ASCE)GM.1943-5622.0000898.

Terzaghi, K. and Peck, R.B. (1948), *Soil Mechanics in Engineering Practice*, John Wiley and Sons, New york.

The Hardening Soil Model-A Practical Guidebook, ZSoil. PC 100701 report, revised 21.10.2018.

Tjie-Liong, G. (2014), "Common mistakes on the application of Plaxis 2D in analyzing excavation problems", *Int. J. Appl. Eng. Res.*, **9**, 8291-8311.

Uncuoglu, E., Laman, M., Saglamer, A. and Kara, H.B. (2008), "Prediction of lateral effective stresses in sand using artificial neural network", *Soils Found.*, **48**(2), 141-153. https://doi.org/10.3208/sandf.48.141.

Uncuoğlu, E. (2015), "The bearing capacity of square footings on a sand layer overlying clay", *Geomech. Eng.*, **9**(3), 287-311. https://doi.org/10.12989/gae.2015.9.3.287.

Uncuoğlu, E., Latifoğlu, L. and Özer, A.T. (2021), "Modelling of lateral efective stress using the particle swarm optimization with machine learning models", *Arabian J. Geosci.*, **14**, 2441. https://doi.org/10.1007/s12517-021-08686-9.

Uncuoglu, E., Citakoglu, H., Latifoglu, L., Bayram, S., Laman, M., Ilkentapar, M. and Oner, A.A. (2022), "Comparison of neural network, Gaussian regression, support vector machine, long short-term memory, multi-gene genetic programming, and M5 Trees methods for solving civil engineering problems", *Appl. Soft Comput.*, **129**, 109623. https://doi.org/10.1016/j.asoc.2022.109623.

Vesic, A.S. (1973), "Analysis of ultimate loads of shallow foundations", *J. Soil Mech. Found. Div. ASCE*, **99**(1), 45-73.

Vu Luat, N., Lee, K. and Thai, D.K. (2020), "Application of artificial neural networks in settlement prediction of shallow foundations on sandy soils", *Geomech. Eng.*, **20**(5), 385-397. https://doi.org/10.12989/gae.2020.20.5.385

GC